

AUTOMATIC DELINEATION OF MACULAR REGIONS BASED ON A LOCALLY DEFINED CONTRAST FUNCTION

J. R. Harish Kumar^{1,2}, Rittwik Adhikari³, Yogish Kamath⁴, Rajani Jampala⁴, Chandra Sekhar Seelamantula¹

¹Department of Electrical Engineering, Indian Institute of Science, Bangalore, India

²Department of Electrical and Electronics Engineering, Manipal Institute of Technology, India

³Department of Computer Science and Engineering, PES Institute of Technology, India

⁴Department of Ophthalmology, Kasturba Medical College, Manipal University, India

harish.jr@ee.iisc.ernet.in, chandra.sekhar@ee.iisc.ernet.in,

rittwik.adhikari@gmail.com, yogish.kamath@manipal.edu, dr.rjny.j@gmail.com

ABSTRACT

We consider the problem of fovea segmentation and develop a technique for delineation of macular regions based on the active-disc formalism that we recently introduced. The outlining problem is posed as one of the optimization of a locally defined contrast function using gradient-ascent maximization with respect to the affine transformation parameters that characterize the active disc. For automatic localization of the fovea and initialization of the active disc, we use the directional-derivative-based matched filter. We report validation results on three publicly available fundus image databases, amounting to a total of 1370 fundus images for automatic fovea localization and 370 fundus images for fovea segmentation and macular regions delineation. The proposed method results in a fovea localization accuracy of 100%, 92%, and 99.4%, and an average Dice similarity index of 77.78%, 67.46%, and 76.56% on DRIVE, DIARETDB0, and MES-SIDOR fundus image databases, respectively. We have also developed an ImageJ plugin and an iOS App based on the proposed method.

Index Terms— Segmentation, fovea, macular regions, maculopathy, active disc, fundus images

1. INTRODUCTION

The macula is a central area in the retina of the human eye. The center of the macula is called the fovea and is responsible for central, high-resolution vision. The macula is subdivided into regions called foveal avascular zone (FAZ), fovea, parafovea, and perifovea [1]. The foveal avascular zone can further be subdivided into umbo and foveola regions. Figure 1 shows the retinal fundus image, with the different regions of the macula outlined. These regions are described and delineated on the basis of histological findings [2]. They are

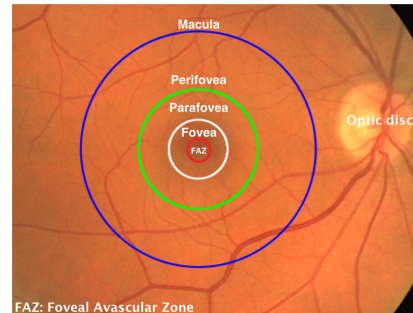


Fig. 1. Histology based delineation of macular regions.

hard to differentiate using a fundus image of the retina. Certain pathological conditions of the macula such as age-related macular degeneration (AMD), diabetic macular edema, macular hole, and macular pucker can affect the macula and, in turn, one's central vision.

Maculopathy is one of the leading causes of vision loss [3]. For identification of the stage and severity of maculopathy, it is important to segment the fovea and its surrounding regions within the macula. Fundus imaging machines are an effective tool for diagnosing retinal diseases such as maculopathy, but there is a lack of robust, semi-automated or automated disease diagnosis tools. Some efforts have been made to develop an automated or semi-automated technique for reliable segmentation of fovea followed by macular region delineation and subsequent diagnosis of the stage and severity of maculopathy. In this paper, we develop a fully automated technique for segmentation and delineation of macular regions using retinal fundus images, which is a precursor and an important step in the severity grading of maculopathy.

1.1. State of the Art

Several efforts have gone into segmenting and delineating the macular regions. Punnolil [4] and Medhi and Dandapat [5] di-

This work was supported by the Ministry of Human Resource Development under the IMPRINT India Initiative (Domain: Healthcare).

vided the macula into three circular regions depending on ratios of one-third, one, and twice the optic disc diameter. Lim et al. [6] segmented the macula into two circular regions. In these methods, concentric circles are drawn at the fovea center, which is detected at a distance about two times the optic disc diameter temporal to the optic disc. The optic disc diameter is an essential parameter in their methods. These methods are dependent on accurate optic disc segmentation, but not on the actual topography of the macula. Some methods have addressed the issue of fovea localization only [7], [8], [9], [10], and [11]. The optic disc location information was used to localize the fovea in [7], [8], and [9]. Lu and Lim's line-operator-based method makes use of the circular brightness profile of the macula [10]. Niemeijer et al. [11] first detect the fovea center and estimate the fovea (clinician macula) as a circle of 50 pixels radius. The problem of fovea segmentation and macular region delineation based on its actual topography using fundus images has not been addressed in the literature. However, several methods have been proposed for macular layer segmentation based on optical coherence tomography (OCT) images [12–15].

1.2. Our Contribution

The difficulty in segmenting the macula into various regions arises because the regions do not have well defined boundaries. In this paper, we introduce a novel, automated, and active-disc-based method for fovea segmentation and macular region delineation. In [16], we introduced the active disc methodology for segmenting the optic disc in fundus images. Our methodology is based on the unified formulation reported in [17], which generalized the approach presented in [18]. During segmentation, a template disc is evolved from a specified initialization towards the boundary of the fovea by maximizing a local energy function that measures the local contrast. The disc evolution is based on a restricted affine transformation that allows for translation and isotropic scaling. Since the contour is constrained to be circular, rotation is not considered and the scaling is made isotropic. The three parameters (the coordinates of the center and the isotropic scale parameter) are optimized for using a standard gradient-ascent optimizer [19]. In order to make the calculations computationally efficient, we use Green's theorem [20]. For automatic localization of the fovea, we use the directional-derivative-based matched filtering technique [21]. Finally, the algorithm performance is assessed by comparing the algorithm outlining with that given by two expert ophthalmologists. For quantitative comparison, we use the Dice index as the metric [22]. Finally, for delineating the macular regions, we use the macular structural information and histology [1], [2]. Concentric circles delineating the anatomical macular regions are drawn with the center of the fovea as the common center, following the ratio of diameters as prescribed in [2]: macula : parafovea : fovea : FAZ = 5.5 : 2.5 : 1.5 : 0.5.

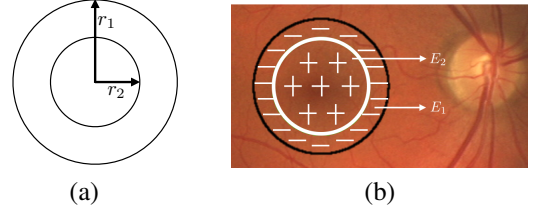


Fig. 2. [Color online] (a) An active disc template; and (b) Optimal active disc fit on the fovea. The white contour is the fovea outline, and the black contour is used for computing the local contrast.

2. ACTIVE DISC FORMULATION AND OPTIMIZATION

An active disc template consists of a pair of concentric circles, and is subjected to a specific affine transformation that allows only for translation and isotropic scaling. The translation and scaling parameters are chosen to optimize a local contrast function. In [16], we introduced the active disc technique to segment the optic disc in retinal fundus images. In this paper, we use the active disc technique to perform fovea segmentation and subsequent macular region delineation in fundus images.

Template Parametrization: The template consists of a pair of concentric circles with center at the origin and the radii of the outer and inner circles, \$r_1 = 1\$ and \$r_2 = 1/\sqrt{2}\$, respectively. Parametric equations defining the template are given as: \$x_i(t) = r_i \cos t\$ and \$y_i(t) = r_i \sin t\$, for \$i = 1, 2\$, and \$\forall t \in (0, 2\pi]\$. An example of such a template is shown in Fig. 2(a). For brevity of notation, we denote \$(x_i(t), y_i(t))\$ as \$(x_i, y_i)\$.

From Template to Active Disc: An active disc is obtained from the template by means of the following transformation: \$X_i = Rx_i + x_c\$ and \$Y_i = Ry_i + y_c\$, \$i = 1, 2\$; \$(X_1, Y_1)\$, and \$(X_2, Y_2)\$ are the outer and inner contours, respectively, of the active disc. The center of the active disc is at \$(x_c, y_c)\$, which is the translation parameter; \$R\$ is the scale parameter. Note that \$X_1, X_2, Y_1\$, and \$Y_2\$ are functions of \$t\$. The inner circle is the desired contour and the outer circle serves as a reference to compute the local contrast.

Active Disc Energy: We consider the region enclosed by the inner circle as the foreground (denoted as \$\mathcal{R}_2\$) and that in the annulus between the inner and outer circles as the immediate background (denoted as \$\mathcal{R}_1 - \mathcal{R}_2\$, where \$\mathcal{R}_1\$ is the region enclosed by the outer circle). The disc energy is defined as the normalized contrast function: \$E = -\frac{1}{R^2}(E_1 - 2E_2)\$, where \$E_i = \iint_{\mathcal{R}_i} f(X, Y) dX dY\$, \$i = 1, 2\$, and \$f\$ is the given two-dimensional (2-D) function (which, in the present case, is the grayscale representation of the fundus image). By maximizing the energy \$E\$ with respect to scale parameter \$R\$ and trans-

lation parameters x_c and y_c , the active disc can be made to lock on to the parafovea. The normalization by R^2 ensures that among all competing candidates with the same contrast $E_1 - 2E_2$, the tightest fit outline is obtained. An example of an optimal active disc with corresponding regional energies indicated is shown in Fig. 2(b).

Optimization: In order to optimize E with respect to the parameters R , x_c , and y_c , we use the gradient-ascent technique, which is a first-order optimization algorithm to find local maximum. We found that the first-order technique suffices although one could use a second-order method. The step value γ_n in every iteration is proportional to the positive of the gradient of the function. One starts with an initial guess P_0 for a local maximum of $E[P_0]$, and considers the sequence P_0, P_1, P_2, \dots such that,

$$P_{n+1} = P_n + \gamma_n \nabla E[P_n]; \quad E[P_0] \leq E[P_1] \leq E[P_2] \dots,$$

where P_n denotes the parameter (R , x_c , or y_c) at iteration n . Gradient-ascent optimization requires the partial derivatives of the energy function. Since the integrals are two-dimensional and the contours are closed, one could compute the partial derivatives efficiently using Green's theorem. The details are available in [16]. The final expressions are reproduced below:

$$\begin{aligned} \frac{\partial E}{\partial R} &= \frac{1}{R} \left(\int_{t=0}^{2\pi} f(X_1, Y_1) dt - \int_{t=0}^{2\pi} f(X_2, Y_2) dt - 2E \right), \\ \frac{\partial E}{\partial x_c} &= \frac{1}{R^2} \left(\int_{t=0}^{2\pi} (\sqrt{2}f(X_1, Y_1) dt - 2f(X_2, Y_2)) \cos t dt \right), \\ \frac{\partial E}{\partial y_c} &= \frac{1}{R^2} \left(\int_{t=0}^{2\pi} (\sqrt{2}f(X_1, Y_1) dt - 2f(X_2, Y_2)) \sin t dt \right). \end{aligned}$$

The active disc is initialized automatically by using the high intensity point resulting from directional-derivative-based matched filtering technique. The initialized disc is allowed to evolve until a suitable convergence criterion is met. The contour marked in white shows the fovea outline.

3. MACULAR REGION DELINEATION

The macula consists of the FAZ, the fovea, and the parafoveal and perifoveal regions, which are annular. The terms used to describe the macular regions differ between the histologist and the clinician. The histologist uses the term fovea to describe what a clinician would name macula, and the term foveola to describe what a clinician would name the fovea. There is no universal agreement regarding its definition, and its usage varies from one clinician to another [2]. In this paper, we have adopted the histological characterization of the macula, because it is more suitable for severity grading of maculopathy. The diameters in millimeters of the anatomical macula and its regions are given as follows — macula : parafovea : fovea : FAZ = 5.5 : 2.5 : 1.5 : 0.5 [2]. Since, our

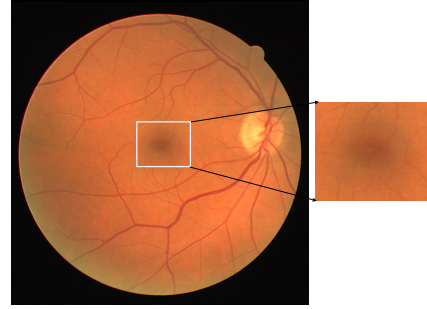


Fig. 3. Fovea template cropped from a fundus image.

active disc segments and outlines the fovea, we took the diameter of the fovea as the reference for delineating the other regions, and consequently maintain the following ratio of diameters — macula : parafovea : fovea : FAZ = 3.67 : 1.67 : 1.0 : 0.33. The following equation gives outlines of perifovea, parafovea, fovea, and FAZ, with the optimized active disc center as the center of all concentric circles: $(x - x_c)^2 + (y - y_c)^2 = (\alpha R)^2$, where R is the active disc radius (upon convergence, the active disc latches on to the fovea), and $\alpha = 3.67, 1.67, 1.0, \text{ and } 0.33$ for perifovea, parafovea, fovea, and FAZ, respectively.

4. AUTOMATIC LOCALIZATION

Automatic detection is an important step in screening applications. Fovea localization is often linked to detection of the main artery and optic disc. These features may not always be captured reliably by the fundus imaging device. Algorithms are required to determine the optic disc accurately together with the segmentation of arteries. This process is lengthy and adds to the time required to localize the fovea. We perform fovea localization using directional-derivative-based matched filtering technique. We use a natural fovea template obtained by cropping out a distinguishable fovea from a good retinal fundus image (cf. Fig. 3). We obtain the Sobel-filter-based directional derivative of the fundus image and fovea template, which, in turn, are used for fovea localization using matched filtering. For the fundus image databases used, we have found that a Sobel mask of size 15×15 highlights the fovea. For smaller mask sizes, the fovea was not prominent and for bigger mask sizes, the fovea was dominated by noise. The matched filter response at (x_p, y_p) is given by $s(x_p, y_p) = \iint f_I(x, y) m(x - x_p, y - y_p) dx dy$, where $f_I(x, y)$ and $m(x, y)$ are the Sobel-transformed fundus image and fovea template, respectively. The peak in the cross-correlation is taken for localizing the fovea and for initializing the active disc. This technique does not rely on optic disc detection nor segmentation of blood vessels.

Table 1. Comparison of Fovea Localization Accuracy

| Method | Database (# fundus images) | Detection accuracy |
|--------------------------|---|----------------------|
| Sinhanayothin et al. [7] | Local (112) | 80.4% |
| Niemeijer et al. [11] | Local (600) | 94.4% |
| Marino et al. [8] | Local (135) | 93.33% |
| Zhang et al. [21] | Local (139) | 98.1% |
| Medhi et al. [5] | DRIVE, Aria, and DIARETDB1 (50 images chosen) | 100% |
| Proposed method | DRIVE (40) DIARETDB0(130) MESSIDOR(1200) | 100% 92% 99.4% |

5. EXPERIMENTAL RESULTS

We developed an ImageJ [23] plugin to implement the proposed method for fully automated fovea localization followed by segmentation and macular region delineation based on a histological characterization. The method has been validated on DRIVE [24], DIARETDB0 [25], and MESSIDOR [26] databases, which are publicly available fundus image databases. The test images are coupled with fovea ground-truth information labelled anonymously by the third and fourth authors of this paper, who are practicing ophthalmologists. The algorithm outlines were not made available to them. The active disc is initialized automatically using the directional-derivative-based matched filtering technique described in Section 4. When the active disc energy function is maximized, the active disc locks on to the dark region. Figures 4(a1)–(a2) and 4(b1)–(b2) show the fundus images with expert and algorithm outlining of the fovea, respectively. Figures 4(c1)–(c2) show the macular regions delineated according to the histological nomenclature of the macula. The performance of the method is quantified using the Dice index, which measures the degree of similarity between two given regions. When the Dice index is 100%, there is perfect agreement between the expert and algorithm outlines. In Table 1, we present the fovea localization accuracy of the proposed method and performance comparison with other state-of-the-art techniques. In Table 2, Dice index values obtained for three publicly available fundus image databases are given. Our technique results in fovea localization accuracies of 100%, 92%, and 99.4%, together with Dice indices of 77.78 %, 67.46%, and 76.56% on DRIVE, DIARETDB0, and MESSIDOR fundus image databases, respectively. Segmentation of fovea and subsequent macular regions delineation is a hard problem, as its borders are not well defined in color fundus photographs. The Dice index obtained suggests that the algorithm outlining has a higher degree of agreement with the expert outlines over several images. We are unable to provide the results for the other methods as their implemen-

Table 2. Performance Analysis of the Active Disc Method

| Database | # fundus images | Average Dice index |
|-----------|-----------------|--------------------|
| DRIVE | 40 | 77.78% |
| DIARETDB0 | 130 | 67.46% |
| MESSIDOR | 200 | 76.56% |

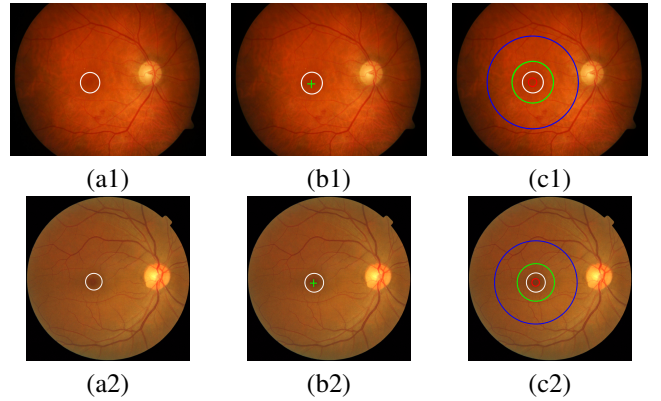


Fig. 4. [Color online] Macular region outlines on fundus images. (a1)–(a2): fovea marked (in white) by an expert; (b1)–(b2): Fovea localization (green +) and algorithm outline of the fovea (white), and (c1)–(c2): algorithm based macular region delineation (FAZ – red, fovea – white, parafovea – green, perifovea – blue).

tations are not publicly available. In addition, in keeping with the contemporary trend of developing smartphone-based eye-care solutions, we have developed an iOS App for real-time implementation of the proposed method. We hope that this will be an effective tool for prescreening. The plugin and App will be made available on request. Snapshots of the ImageJ plugin and iOS App are available at [27].

6. CONCLUSIONS

We proposed an active-disc-based segmentation technique for delineating macular regions (characterized based on histology) in retinal fundus images, which is a precursor and important step in the automated diagnosis and severity grading of maculopathy. The localization of the fovea and subsequent initialization of the active disc on the region of interest is performed with directional-derivative-based matched filtering technique. The translation and scale parameters of the active disc are optimized with the local contrast as the energy function. The optimization is carried out using gradient-ascent technique and the partial derivatives are evaluated using Green’s theorem. The fovea segmentation performance was found to be in good agreement with the expert outlines over a large number of images taken from three publicly available fundus image databases.

7. REFERENCES

- [1] Interpretation of Stereo Ocular Angiography – Retinal and Choroidal Anatomy: http://www.cybersight.org/bins/content_page.asp.
- [2] L. A. Remington, *Clinical Anatomy and Physiology of the Visual System*. Elsevier Butterworth-Heinemann Inc., Third Ed., pp. 83–86, 2012.
- [3] Global data on visual impairments 2010 – World Health Organization:
- [4] A. Punnolil, “A novel approach for diagnosis and severity grading of diabetic maculopathy,” in *Proc. Intl. Conf. on Advances in Computing, Communications and Informatics*, pp. 1230–1235, 2013.
- [5] J. P. Medhi and S. Dandapat, “Analysis of maculopathy in color fundus images,” in *Proc. 2014 IEEE India Conference*, pp. 1–4, 2014.
- [6] S. T. Lim, W. M. D. W. Zaki, A. Hussain, S. L. Lim, and S. Kusalavan, “Automatic classification of diabetic macular edema in digital fundus images,” in *Proc. IEEE Colloquium on Humanities, Science and Engineering*, pp. 265–269, 2011.
- [7] C. Sinthanayothin, J. F. Boyce, H. L. Cook, and T. H. Williamson, “Automated localisation of the optic disc, fovea, and retinal blood vessels from digital colour fundus image,” in *British Journal of Ophthalmology*, vol. 83, pp. 902–910, 1999.
- [8] C. Marino, S. Pena, M. G. Penado, M. Ortega, J. Rouco, A. Pose-Reino, and M. Pena, “Macula precise localization using digital retinal angiographies,” in *WSEAS Trans. Computer Research*, pp. 43–50, 2008.
- [9] K. W. Tobin, E. Chaum, V. P. Govindasamy, and T. P. Karnowski, “Detection of anatomic structures in human retinal imagery,” in *IEEE Trans. Medical Imaging*, vol. 26, no. 12, pp. 1729–1739, 2007.
- [10] S. Lu and J. H. Lim, “Automatic macula detection from retinal images by a line operator,” in *Proc. IEEE Intl. Conf. on Image Processing*, pp. 4073–4076, 2010.
- [11] M. Niemeijer, M. D. Abramoff, and B. V. Ginneken, “Segmentation of the optic disc, macula and vascular arch in fundus photographs,” *IEEE Trans. on Medical Imaging*, vol. 26, no. 1, pp. 116–127, 2007.
- [12] H. Ishikawa et al., “Macular segmentation with optical coherence tomography,” *Invest. Ophthalmol. Visual Sci.*, vol. 46(6), pp. 2012–2017, 2005.
- [13] T. Fabritius et al., “Automated segmentation of the macula by optical coherence tomography,” *Opt. Express*, vol. 17(18), pp. 15659–15669, 2009.
- [14] Q. Yang et al., “Automated layer segmentation of macular OCT images using dual-scale gradient information,” *Opt. Express*, vol. 18(20), pp. 21293–21307, 2010.
- [15] X. Zhang, S. Yousefi, L. An, and R. K. Wang, “Automated segmentation of intramacular layers in Fourier domain optical coherence tomography structural images from normal subjects,” *Journal of Biomedical Optics*, vol. 17(4), pp. 046011– to 1046011–7, 2012.
- [16] J. R. Harish Kumar, A. K. Pediredla, and C. S. Seelamantula, “Active discs for automated optic disc segmentation,” in *Proc. IEEE Global Conf. on Signal and Information Processing*, pp. 225–229, 2015.
- [17] A. K. Pediredla and C. S. Seelamantula, “A unified approach for optimization of snakuscules and ovuscules,” in *Proc. IEEE Intl. Conf. on Acoustics, Speech, and Signal Processing*, pp. 681–684, 2012.
- [18] P. Thévenaz and M. Unser, “Snakuscules,” *IEEE Trans. on Image Processing*, vol. 17, no. 4, pp. 585–593, 2008.
- [19] E. K. P. Chong and S. H. Zak, *An Introduction to Optimization*. Wiley-Interscience, Second Ed., pp. 115–134, 2001.
- [20] G. F. Simmons, *Calculus with Analytic Geometry*. The McGraw-Hill Companies, Inc., Second Ed., pp. 764–770, 1996.
- [21] B. Zhang and F. Karay, “Optic disc and fovea detection via multi-scale matched filters and a vessel’s directional matched filter,” in *Proc. Intl. Conf. on Autonomous and Intelligent Systems*, pp. 1-5, 2010.
- [22] W. R. Crum, O. Camara, and D. L. G. Hillu, “Generalized overlap measures for evaluation and validation in medical image analysis,” *IEEE Trans. Medical Imaging*, vol. 25, no. 11, pp. 1451–1461, 2006.
- [23] ImageJ: <http://www.imagej.nih.gov/ij/>
- [24] DRIVE Database: <http://www.isi.uu.nl/Research/Databases/DRIVE/>
- [25] DIARETDB0 Database: <http://www.it.lut.fi/project/imageret/diaretdb0/>
- [26] MESSIDOR Database: <http://www.adcis.net/en/Download-Third-Party/Messidor.htmlindex-en.php>
- [27] <https://sites.google.com/site/chandrasekharseelamantula/>